

1960  
TECHNISCHE HOGESCHOOL DELFT  
VLIEGTUIGBOUWKUNDE  
BIBLIOTHEEK

CoA REPORT AERO. NO. 188

TECHNISCHE UNIVERSITEIT DELFT  
LICHTVAART- EN RUIMTEVAARTECHNIEK  
BIBLIOTHEEK  
Kluivenweg 1 - 2629 HS DELFT



THE COLLEGE OF AERONAUTICS  
CRANFIELD

A METHOD OF PREDICTING THE AERODYNAMIC BLOCKAGE  
OF BLUFF BODIES IN A DUCTED AIRSTREAM

by

A. H. Lefebvre

November, 1965

THE COLLEGE OF AERONAUTICS  
CRANFIELD

A Method of Predicting the Aerodynamic Blockage  
of Bluff Bodies in a Ducted Airstream

- by -

A.H. Lefebvre, B.Sc. (Mech. Eng.), D.I.C., Ph.D.,  
M.I. Mech.E., A.F.R.Ae.S.

SUMMARY

Consideration is given to the flow conditions in the vicinity of a bluff body immersed in a ducted airstream. By equating the pressure loss expressed in terms of drag coefficient and physical blockage to the pressure loss occurring in the flow expansion downstream of the plane of maximum aerodynamic blockage, a relationship between geometric and aerodynamic blockage is obtained of the form

$$\left[ \frac{1}{(1 - B_a)^2} - 1 \right] = \phi \frac{B_g}{(1 - B_g)^2}$$

where  $B_g$  is the geometric blockage,  $B_a$  is the aerodynamic blockage and  $\phi$  is a function of the drag coefficient. It is argued that for any given body shape  $\phi$  is constant, and supporting experimental evidence is presented which shows, in addition, that for circular cones with apex pointing upstream,  $\phi = 0.44 \left( \sin \frac{\theta}{2} \right)^{0.5}$ ,  $\theta$  being the included angle of the cone.

## CONTENTS

	<u>Page</u>
Summary	
List of Symbols	
1. Introduction	1
2. Theory	2
3. Comparison with experiment	4
4. Application to other bluff body shapes	5
5. Previous work	6
6. Conclusions	7
References	9
Table	9
Figures	

## LIST OF SYMBOLS

d	maximum diameter or width of recirculation zone
$A_s$	maximum cross-sectional area of recirculation zone
A	cross-sectional area of closed duct
a	maximum cross-sectional area of bluff body
$\ell$	gas density
V	gas velocity
D	dynamic head, $0.5 \ell V^2$
p	static pressure
$\Delta p$	static pressure change
$C_D$	drag coefficient for zero blockage
$C_{D_B}$	corresponding base drag coefficient
$B_g$	maximum geometric blockage
$B_a$	maximum aerodynamic blockage
n	index of d in stability correlation
$\eta_{diff}$	diffusion efficiency
$\phi$	$C_D (1 - \eta_{diff})^{-1}$
$\theta$	included angle of cone

## SUFFICES

1	denotes conditions upstream of bluff body
2	denotes conditions in plane of maximum physical blockage
3	denotes conditions in plane of maximum aerodynamic blockage
4	denotes conditions downstream of the recirculation zone

## 1. Introduction

Flow around a bluff body immersed in an airstream is characterized by the formation of a closed "bubble" behind the body as illustrated in the photograph of Fig. 1. Within the bubble is a region of circulatory flow, whose boundary may be defined as the locus of all points at which the flow subdivides into air which subsequently participates in the circulatory flow and air which proceeds normally downstream. Usually the maximum width of the recirculation zone exceeds that of the body by an amount which depends on the shape of the body and the level of turbulence in the airstream. In the case of an airstream confined to a duct it is also governed by the geometric blockage, i. e. by the ratio of the cross-sectional area of the body to the flow area of the duct. This is because with flow in a duct the rigid walls impede the free movement of air over the body and, in consequence, the axial velocity in its vicinity is higher than it would be if the body were located in an unlimited stream. The effect of this high axial velocity is firstly, to increase the aerodynamic drag of the body above the value corresponding to the upstream dynamic head and, secondly, to reduce the width of the recirculation zone. Thus with flow in a duct one has to define two values of blockage: (a) the physical or geometric blockage, which is the ratio of the maximum cross-sectional area of the body to the flow area of the duct, and (b) the aerodynamic blockage, which is the ratio of the maximum cross-sectional area of the recirculation zone to the duct area. It is assumed that in both cases the cross-sectional area is measured in a plane which is normal to the axial flow direction.

At the present time relatively little is known of the relationship between physical and aerodynamic blockage, although such knowledge would have useful practical applications. One example arises in the design of reheat or afterburner systems for turbojet engines. A reheat system normally comprises a number of bluff body flame stabilizers which are located in the engine tail-pipe. Fuel is injected into the turbine efflux at some plane upstream, and a flame is anchored on the stabilizers from which it can spread to other regions of the tail-pipe. Now the effectiveness of a baffle as a flame stabilizer is known to be improved by an increase in baffle size and reduced by an increase in gas velocity. This dependence may be expressed as a stability criterion of the form

$$\text{flame stability} = f \left( \frac{d^n}{V} \right)$$

where  $d$  = maximum diameter or width of recirculation zone

and  $V$  = local gas velocity

$n$  = constant. Values of  $n$  ranging from 0.5 to 1.0 are reported in the literature

Fig. 2 shows the results of calculations on the variation of  $\frac{d^n}{V}$  with blockage for values of  $n$  of 0.5, 0.75 and 1.0. All three curves exhibit an increase in stability with increase in blockage until a maximum value is reached. Beyond this any possible increase in stability due to an increase in recirculation zone width is more than offset by the corresponding increase in local gas velocity. Thus for any given stabilizer configuration there is an optimum value of blockage for maximum stability.

Fig. 2 shows that for values of  $n$  of 0.5, 0.75 and 1.0 the optimum values of aerodynamic blockage are 0.200, 0.273 and 0.333 respectively. However, even if the designer knows the appropriate value of  $n$ , he is still faced with the difficulty of trying to estimate the stabilizer size required to create the optimum value of aerodynamic blockage. The object of the present investigation is to assist the designer in this problem by providing means whereby, for any given bluff body shape, a quantitative relationship between physical and aerodynamic blockage may readily be found.

## 2. Theory

The following simple theory employs the normal gas dynamic relationships of incompressible flow. Errors due to compressibility effects are considered negligibly small for the velocities encountered in conventional reheat systems which normally do not exceed Mach 0.4.

The notational diagram of Fig. 3 represents a symmetrical bluff body located on the axis of a straight walled duct of uniform cross-sectional area,  $A$ . Attention is focussed on the following flow regimes -

- (1) upstream of the bluff body
- (2) in the plane of maximum geometrical blockage
- (3) in the plane of maximum aerodynamic blockage
- (4) downstream of the recirculation zone.

The pressure loss between planes (1) and (4) may be derived in terms of the drag coefficient and geometric blockage in the following manner.

From momentum considerations we have -

$$p_1 A - p_4 A = C_D \cdot a \cdot D_2 \quad (1)$$

where  $C_D$  = drag coefficient based on zero blockage

$a$  = maximum cross sectional area of bluff body

$$\text{and } D_2 = \frac{1}{2} \rho V_2^2$$

$$\text{or, } \Delta p_{1-4} \cdot A = C_D \cdot a \cdot D_2 \quad (2)$$

$$\begin{aligned} \text{Now, } D_2 &= D_1 \left( \frac{A}{A-a} \right)^2 \\ &= D_1 \left( \frac{1}{1-B_g} \right)^2 \end{aligned} \quad (3)$$

where  $B_g = \frac{a}{A}$  = geometric blockage.

Substitution of (3) into (2) gives

$$\Delta p_{1-4} = D_1 \cdot C_D \cdot \frac{B_g}{(1 - B_g)^2} \quad (4)$$

Equation (4) expresses the overall pressure loss in terms of the upstream dynamic head, the drag coefficient and the geometric blockage. However, one can also write another expression for  $\Delta p_{1-4}$  based on considerations of the flow losses

which occur between these two planes. Between (1) and (3) the flow is contracting, and the only source of pressure loss is that arising from friction along the surface of the bluff body and the duct walls. This loss is relatively small and may reasonably be neglected. There is, however, a reduction in static pressure between planes (1) and (3) due to the increase in air velocity, which is given by Bernoulli's equation as

$$\Delta p_{1-3} = D_1 \left[ \left( \frac{A}{A - A_3} \right)^2 - 1 \right] \quad (5)$$

where  $A_3$  = maximum cross-sectional area of recirculation zone

$$\text{or, } \Delta p_{1-3} = D_1 \left[ \frac{1}{(1 - B_a)^2} - 1 \right] \quad (6)$$

where  $B_a = \frac{A_3}{A}$  = aerodynamic blockage

Downstream of (3) the flow area increases, the velocity decreases and the static pressure rises by an amount which depends on the efficiency at which this diffusion process occurs. If diffusion efficiency is defined in the normal way, we have,

$$\Delta p_{4-3} = \eta \text{ diff } D_4 \left[ \frac{1}{(1 - B_a)^2} - 1 \right]$$

where  $\eta \text{ diff}$  = diffusion efficiency

or, since  $V_4 = V_1$  and hence  $D_4 = D_1$ ,

$$\Delta p_{4-3} = \eta \text{ diff } D_1 \left[ \frac{1}{(1 - B_a)^2} - 1 \right] \quad (7)$$

Now the overall loss in static pressure between (1) and (4) is equal to the fall in static pressure between (1) and (3) minus the gain in pressure resulting from diffusion between (3) and (4)

We have,  $p_1 - p_4 = (p_1 - p_3) - (p_4 - p_3)$

Thus  $\Delta p_{1-4}$  is obtained as the difference between the right hand sides of equations (6) and (7).

$$\text{i.e. } \Delta p_{1-4} = D_1 (1 - \eta \text{ diff}) \left[ \frac{1}{(1 - B_a)^2} - 1 \right] \quad (8)$$

We now have two equations, (4) and (8), for the pressure loss between planes (1) and (4). One, equation (4), is based on the drag coefficient and the geometric blockage,  $B_g$ . The other, equation (8), relates pressure loss to diffusion efficiency and the aerodynamic blockage,  $B_a$ . Equating the two gives

$$D_1 \cdot C_D \cdot \frac{B_g}{(1 - B_g)^2} = D_1 (1 - \eta \text{ diff}) \left[ \frac{1}{(1 - B_a)^2} - 1 \right]$$

or, 
$$\left[ \frac{1}{(1 - B_a)^2} - 1 \right] = \frac{C_D}{(1 - \eta \text{ diff})} \cdot \frac{B_g}{(1 - B_g)^2} \quad (9)$$

### 3. Comparison with experiment

The validity of equation (9) was tested against experimental data obtained by Setarrudin<sup>1</sup> who measured recirculation zone dimensions behind three sets of circular cones of 30°, 45° and 60° included angle. Each set comprised five cones differing in size to give geometric blockages of 0.11, 0.20, 0.31, 0.45 and 0.61. The cones were mounted in turn along the axis of a circular perspex pipe with their apex pointing upstream. Data on the size of the recirculation zone were obtained by water flow visualization techniques, as illustrated in fig. 1, and by a probe method based on the local injection of air bubbles into the water flow at various points downstream of the cone. By gradually increasing the radial protrusion of the probe the boundary of the recirculation zone was defined as the point at which the air bubbles were no longer swept downstream but were entrained into the circulatory flow. Both methods gave almost identical results on the effect of blockage on recirculation zone diameter but with slight differences in absolute values. The present analysis employs the results obtained by the probe method. These are reproduced in fig. 4 and listed in table 1.

Setarrudin's data for the 60° cone are shown in fig. 5 as a plot of

$\left[ \frac{1}{(1 - B_a)^2} - 1 \right]$  against  $\frac{B_g}{(1 - B_g)^2}$ . The result is a straight line through the origin, indicating a constant value for the parameter

$$\frac{C_D}{1 - \eta \text{ diff}} \quad \text{or } \phi.$$

It also implies that the diffusion efficiency remains constant for any given value of  $C_D$  and independent of the blockage. This result is perhaps not too surprising, since although any increase in blockage will increase the area ratio of the diffusing passage and thereby tend to reduce the efficiency, this effect will be counteracted by an increase in efficiency resulting from the corresponding increase in the length of the recirculation zone and hence in the flow length available for diffusion.



Fig. 6 is similar to fig. 5 but also includes Setarrudin's data on 45° and 30° cones. From the slopes of the lines drawn through the experimental points the following results are obtained:-

- for the 60° cone,  $\phi = 3.12$
- for the 45° cone,  $\phi = 2.72$
- for the 30° cone,  $\phi = 2.24$

These results may, incidently, be used to deduce the variation of drag coefficient with cone angle. Fig. 7 shows a plot of  $\log \phi$  against  $\log \sin \frac{\theta}{2}$ ,  $\theta$  being the cone angle. The plotted points lie close to a straight line of slope 0.5, indicating a relationship of the form

$$C_D \propto \left( \sin \frac{\theta}{2} \right)^{0.5} \quad (10)$$

Experimental data obtained by direct measurement on the effect of cone angle on drag coefficient are sparse. For a circular disc, corresponding to a cone angle of 180°, Hoerner<sup>2</sup> quotes a value of  $C_D$  of 1.2. Incorporating this value into equation (10) and substituting into equation (9) yields the following relationships:-

For circular cones with apex pointing upstream

$$C_D = 1.2 \left( \sin \frac{\theta}{2} \right)^{0.5} \quad (11)$$

$$\text{and} \quad \left[ \frac{1}{(1 - B_a)^2} - 1 \right] = 4.4 \left( \sin \frac{\theta}{2} \right)^{0.5} \frac{B_g}{(1 - B_g)^2} \quad (12)$$

where  $\theta$  = cone angle

Equation (12) was used to calculate values of  $B_a$  for all the experimental values of  $\theta$  and  $B_g$  employed by Setarrudin. These 'theoretical' values of  $B_a$  were then plotted against the corresponding experimental values as shown in fig. 8. In this figure the straight line drawn through the origin at 45° to the main axes corresponds to perfect agreement between theory and experiment. The fact that almost all the points fall on or close to this line strongly supports equation (12), which may, therefore, be used with confidence for predicting the aerodynamic blockage created by circular cones.

#### 4. Application to other bluff body shapes

For a bluff body located in a ducted airstream the total drag is composed of the following:-

- (a) forebody drag coefficient
- (b) skin friction drag on body surface
- (c) additional skin friction drag on duct wall due to flow acceleration in vicinity of body.
- (d) base drag coefficient

Of these the component having the most direct influence on the geometry of the recirculation zone is the base drag coefficient,  $C_{DB}$ . For cones and short forebody shapes this is the major component of drag and no great error is incurred if  $C_D$  is used instead of  $C_{DB}$  in calculating  $\phi$ . With long forebody shapes, however, skin friction cannot be neglected and hence  $\phi$  must be calculated on the basis of  $C_{DB}$  only. Moreover, since the diffusion efficiency is determined by the shape of the diffusion passage formed between the recirculation zone and the duct walls, it is to be expected that  $\eta_{diff}$  is also closely related to the base drag coefficient, although with long forebody shapes the boundary layer thickness might also be significant.

The values of  $\phi$  from fig. 6 for  $60^\circ$ ,  $45^\circ$  and  $30^\circ$  cones, when used in conjunction with Hoerner's result of 1.2 for a circular disc ( $180^\circ$  cone), yield a value of  $\eta_{diff}$  of 0.73. For other three-dimensional bodies it is suggested, therefore, that  $\phi$  be calculated using the appropriate value of  $C_{DB}$  and a diffusion efficiency of 0.73.

i. e. for three-dimensional bodies

$$\left[ \frac{1}{(1 - B_a)^2} - 1 \right] = 3.7 \cdot C_{DB} \cdot \frac{B_g}{(1 - B_g)^2} \quad (13)$$

For two-dimensional bodies, in the absence of experimental data from which to deduce the relevant level of diffusion efficiency, recourse must be made to the general equation -

$$\left[ \frac{1}{(1 - B_a)^2} - 1 \right] = \phi \cdot \frac{B_g}{(1 - B_g)^2} \quad (14)$$

If, for any given forebody shape, the relationship between aerodynamic and geometric blockage is known at one value of blockage, this is sufficient to determine  $\phi$  and the above equation may then be used to derive this relationship at any other level of blockage.

## 5. Previous work

Since the present study was completed Maskell<sup>3</sup> has presented a theory of blockage constraint on the flow past a bluff body in a closed wind tunnel. The theory leads to the following 'correction formula'

$$\frac{\Delta q}{q} = \epsilon \cdot C_D \cdot \frac{S}{C} \quad (15)$$

where  $\Delta q$  is the effective increase in dynamic pressure due to constraint, and  $\epsilon$  is a blockage factor dependent on the magnitude of the base-pressure coefficient.  $S$  is the reference area of the model and  $C$  the tunnel cross-sectional area. The factor  $\epsilon$  is shown to be close to 2.5 for aspect ratios in the range 1 to 10.

Although at first sight the above equation may seem unrelated to the present work, by converting velocity ratios into area ratios and changing the notation, it may be rewritten as

$$\left[ \frac{1}{(1 - B_a)^2} - 1 \right] = \epsilon \cdot C_D \cdot B_g \quad (16)$$

as compared with equation (9) which is

$$\left[ \frac{1}{(1 - B_a)^2} - 1 \right] = \frac{C_D}{(1 - \eta \text{ diff})} \cdot \frac{B_g}{(1 - B_g)^2}$$

Apart from differences in derivation the main practical difference between these two expressions is the absence of the term  $(1 - B_g)^2$  in equation (16). This has a negligible effect at the very low values of blockage considered by Maskell, but would lead to appreciable error at high levels of blockage unless, of course, for each value of blockage the appropriate measured or 'corrected' value of  $C_D$  were inserted into the equation.

## 6. Conclusions

(1) For two-dimensional and three-dimensional bluff-bodies located in a closed duct the relationship between geometric and aerodynamic blockage is given by the formula

$$\left[ \frac{1}{(1 - B_a)^2} - 1 \right] = \phi \cdot \frac{B_g}{(1 - B_g)^2}$$

where  $B_g$  = geometric blockage

$B_a$  = aerodynamic blockage

$\phi$  = constant for any given body shape

$$= C_{D_B} / 1 - \eta \text{ diff}$$

(2) For circular cones with apex pointing upstream,

$$\phi = 4.4 \left( \sin \frac{\theta}{2} \right)^{0.5} \text{ and hence}$$

$$\left[ \frac{1}{(1 - B_a)^2} - 1 \right] = 4.4 \left( \sin \frac{\theta}{2} \right)^{0.5} \frac{B_g}{(1 - B_g)^2}$$

(3) For other three-dimensional shapes the following formula is recommended

$$\left[ \frac{1}{(1 - B_a)^2} - 1 \right] = 3.7 \cdot C_{DB} \cdot \frac{B_g}{(1 - B_g)^2}$$

(4) Analysis of the experimental evidence suggests that the drag coefficient of circular cones is proportional to the square root of the sine of the half angle.

$$\text{i.e. } C_D = C_{D 180^\circ} \left( \sin \frac{\theta}{2} \right)^{0.5}$$

where  $C_{D 180^\circ}$  = drag coefficient of circular disc

References

1. Setarrudin, M. Water flow visualization tests on flow past conical baffles. College of Aeronautics Thesis, 1964.
2. Hoerner, F.S. Fluid-dynamic drag. Privately published, New York, 1958.
3. Maskell, E.C. A theory of the blockage effects on bluff bodies and stalled wings in a closed wind tunnel. Published as R. & M. No. 3400 by H.M.S.O., 1965.

TABLE 1

Geometric Blockage  $B_g$	Aerodynamic Blockage, $B_a$		
	60° cone	45° cone	30° cone
0.110	0.155	0.144	0.136
0.200	0.281	0.261	0.246
0.310	0.429	0.402	0.380
0.450	0.580	0.550	0.529
0.610	0.726	0.696	0.675

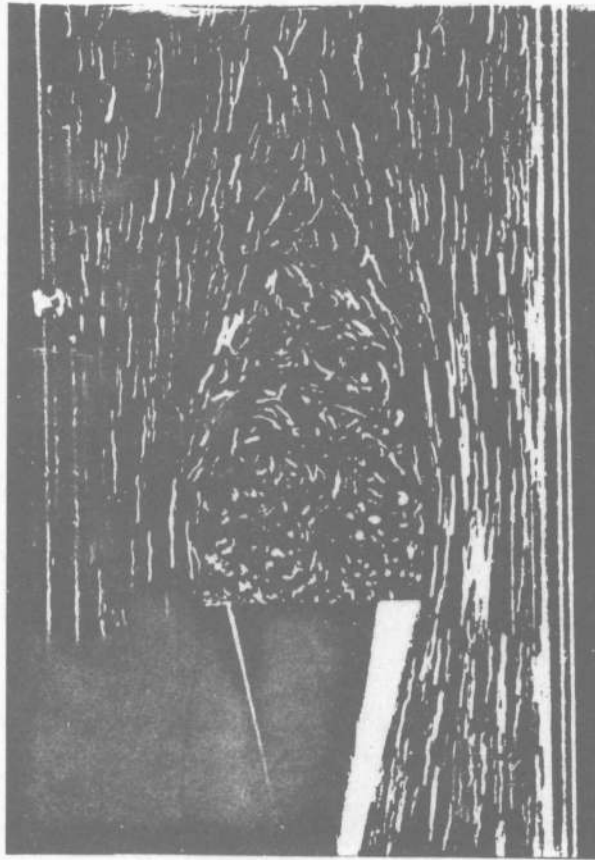


FIG. 1. PHOTOGRAPH ILLUSTRATING FLOW RECIRCULATION ZONE DOWNSTREAM OF A CIRCULAR ZONE

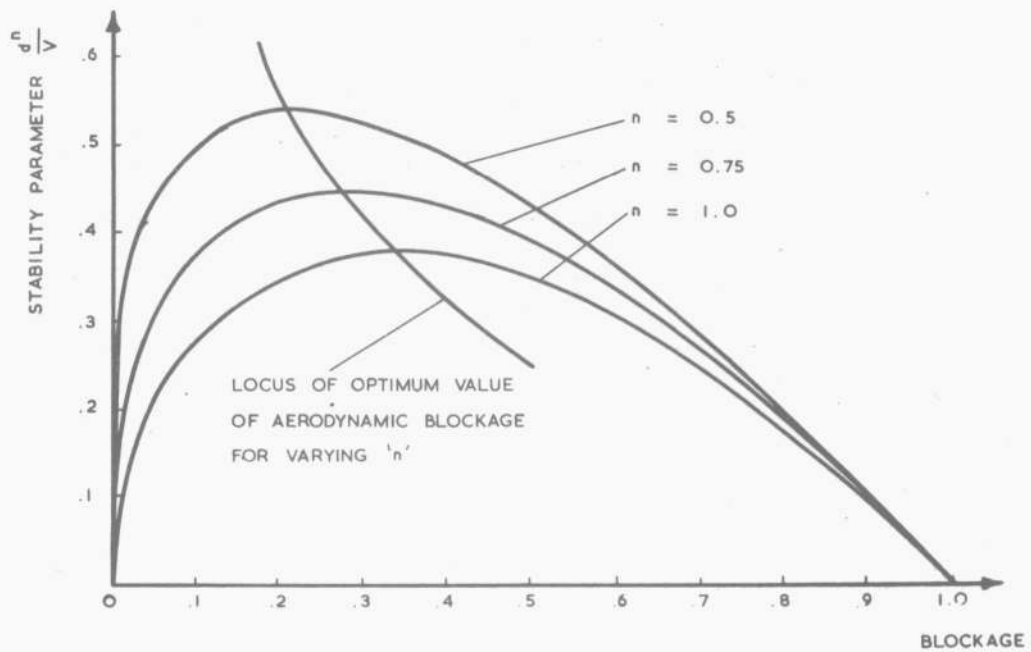


FIG. 2. GRAPHS ILLUSTRATING DEPENDENCE OF FLAME STABILITY ON AERODYNAMIC BLOCKAGE

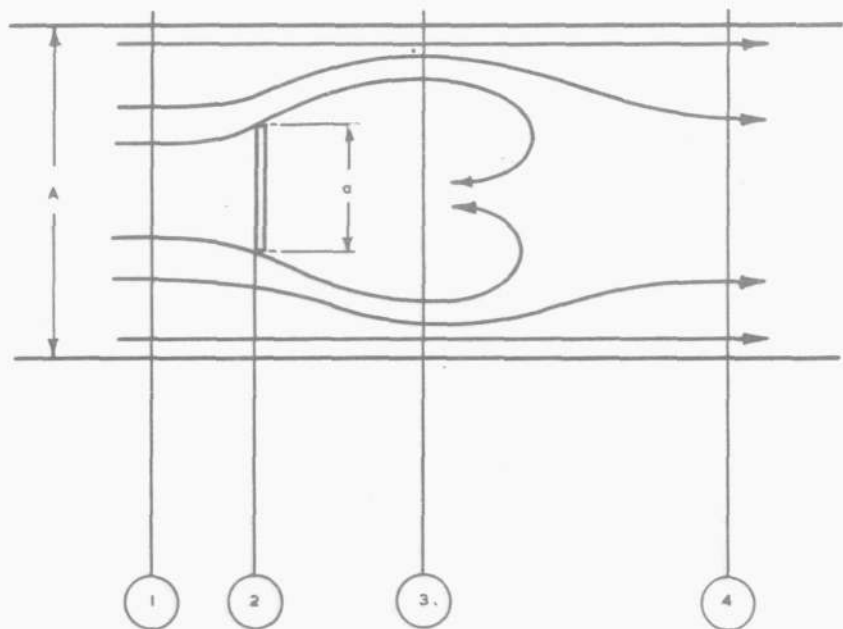


FIG. 3. NOTATIONAL DIAGRAM DENOTING MAIN FLOW REGIMES.

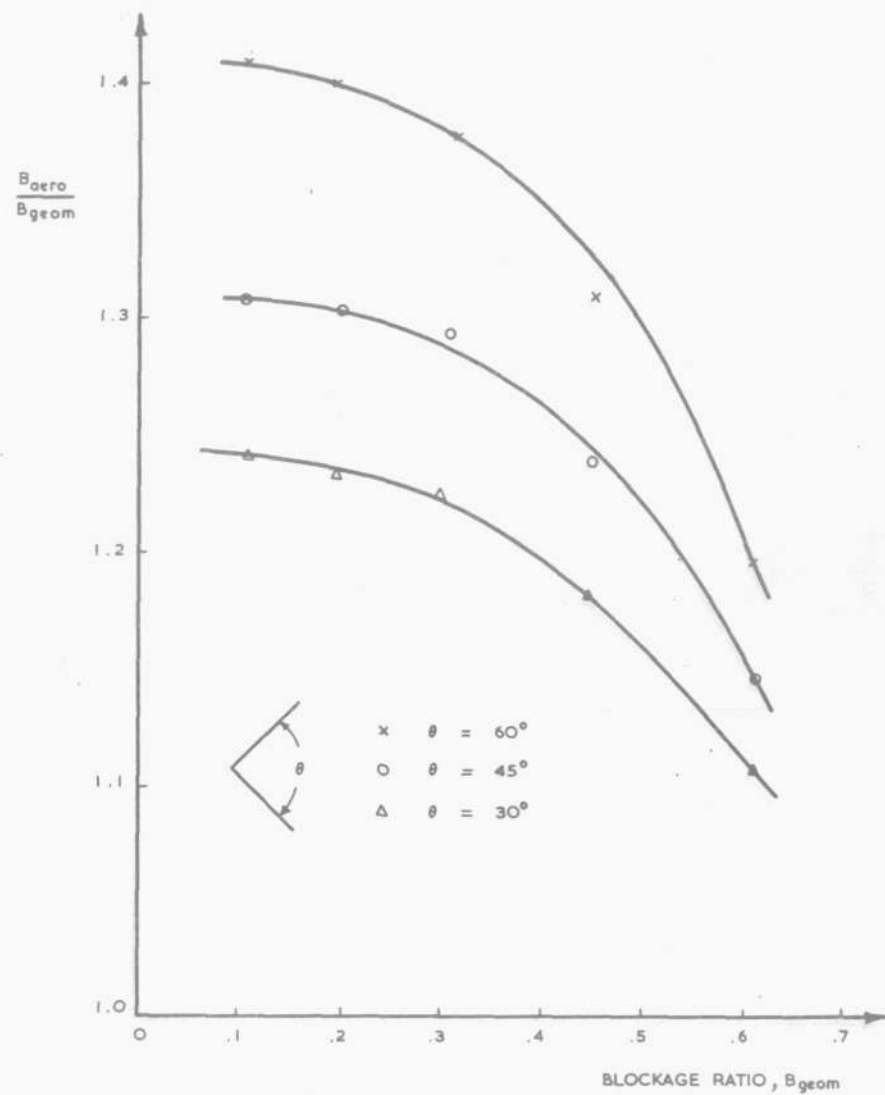


FIG. 4. EXPERIMENTAL DATA ON THE RELATIONSHIP BETWEEN GEOMETRIC AND AERODYNAMIC BLOCKAGE FOR CONES (SETARUDDIN, REF. 1).

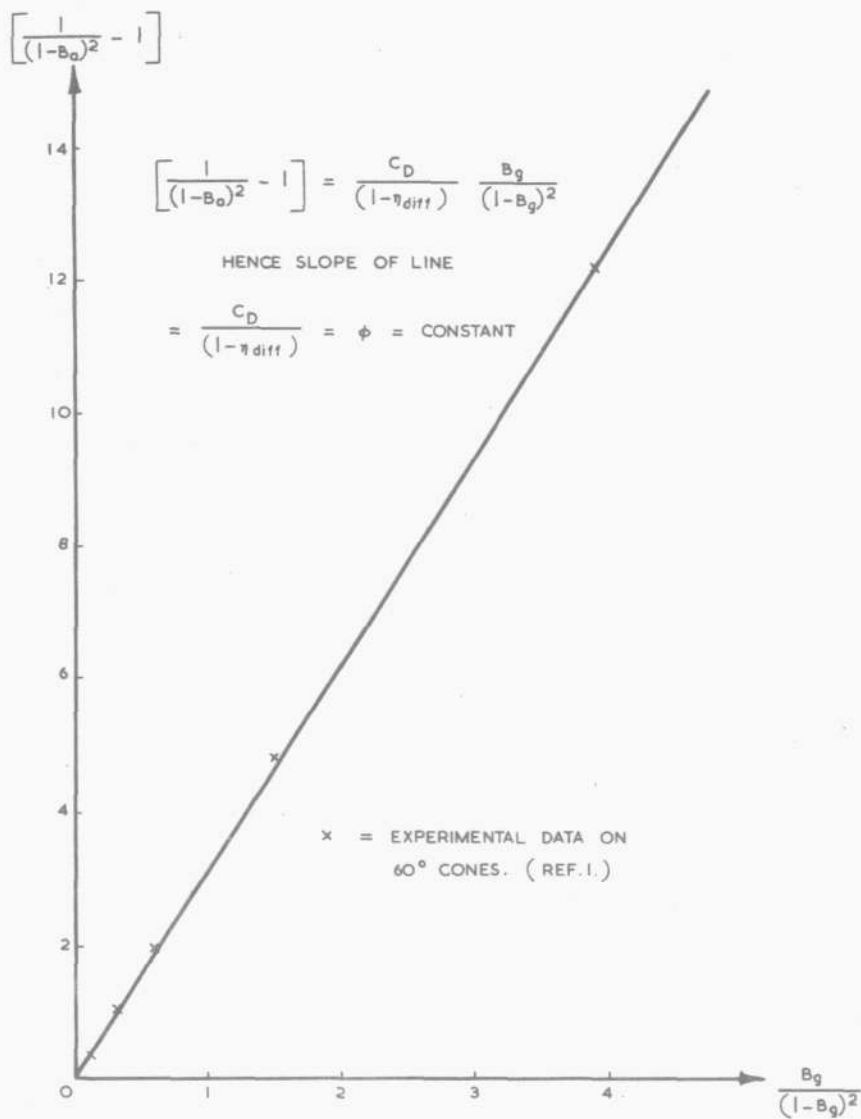


FIG. 5. EXPERIMENTAL SUPPORT FOR CONSTANCY OF  $\phi$  IN EQUATION (9).

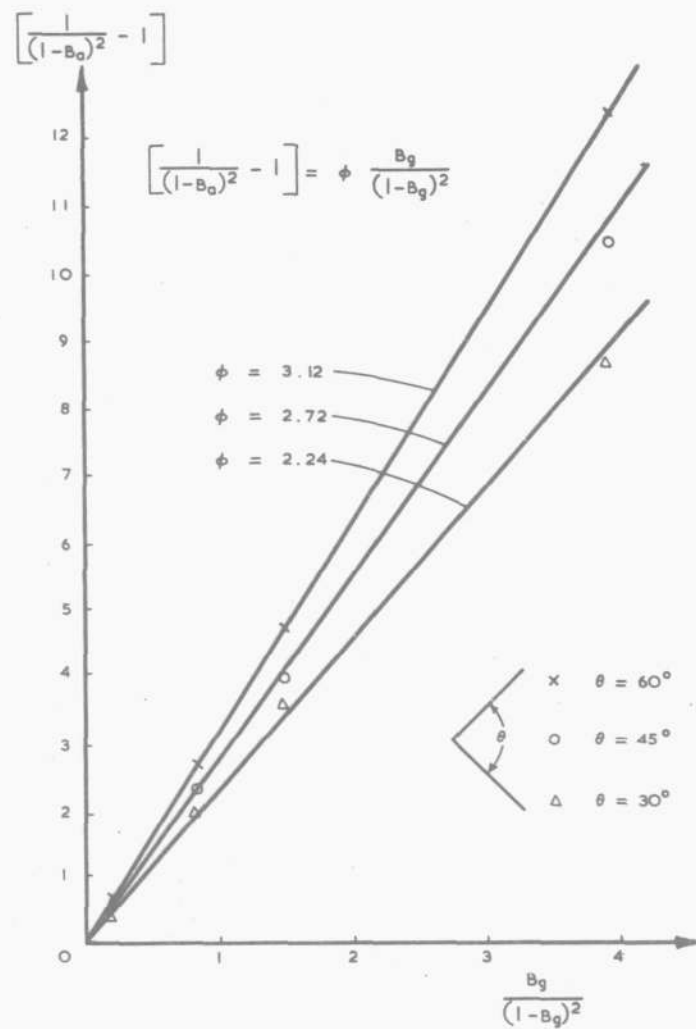


FIG. 6. DETERMINATION OF  $\phi$  FOR CONES.



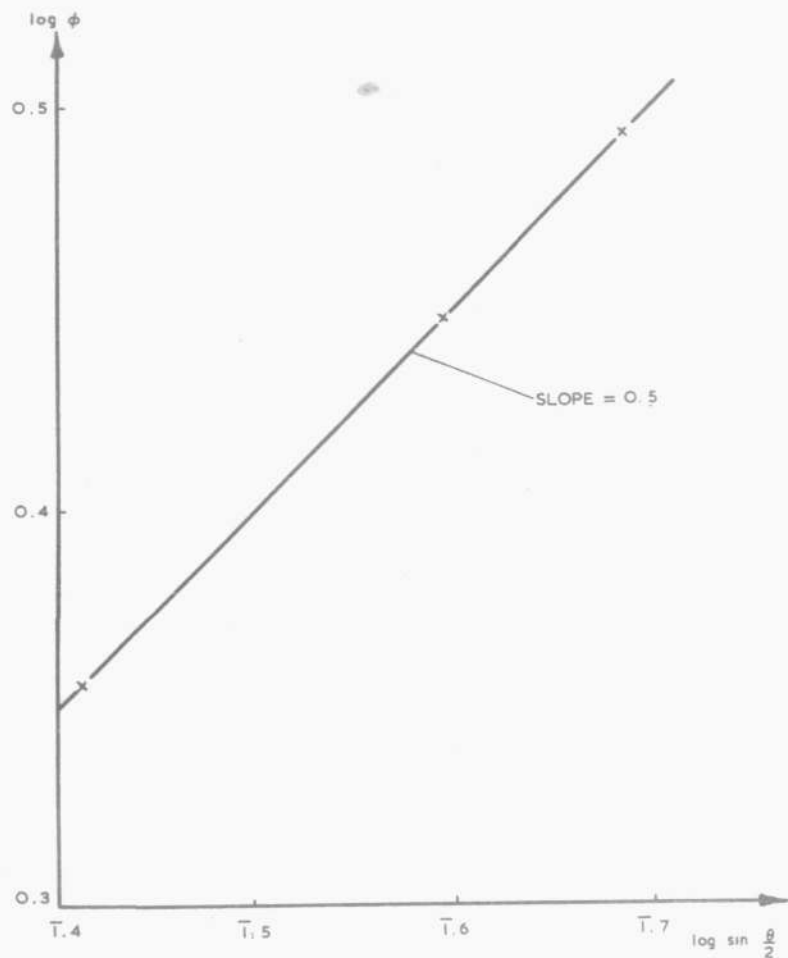


FIG. 7. RELATIONSHIP BETWEEN  $\phi$  AND CONE ANGLE.

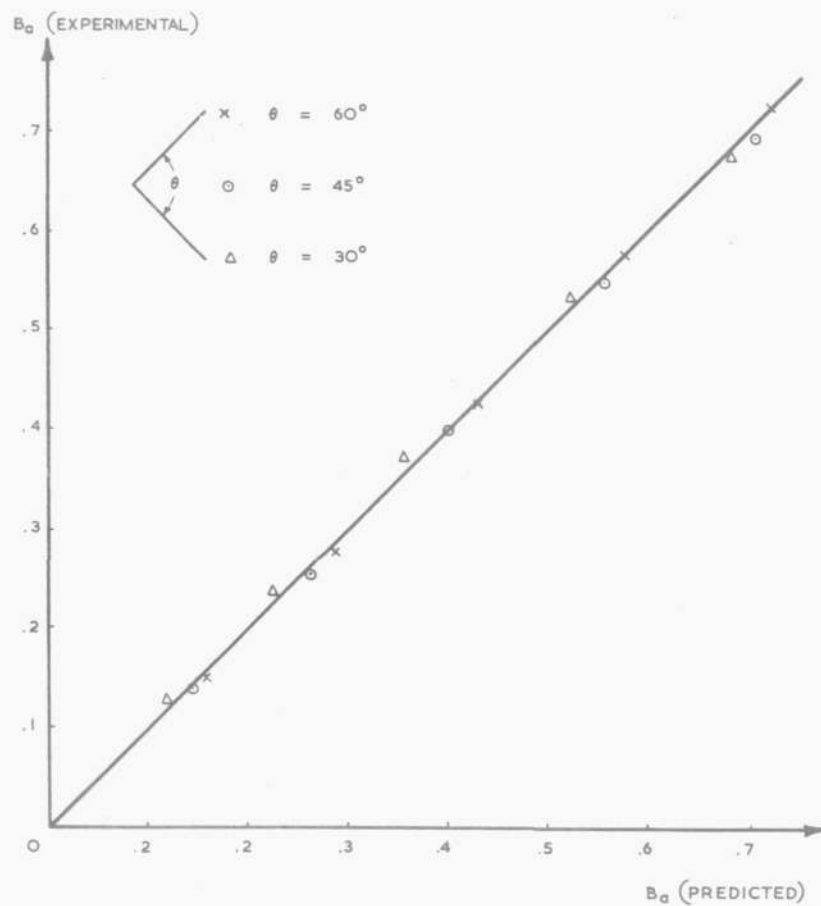


FIG. 8. COMPARISON BETWEEN MEASURED VALUES OF AERODYNAMIC BLOCKAGE AND VALUES PREDICTED FROM EQUATION (12).